Indian J. pure appl. Math., **31**(3) : 227-242, March 2000

MIXED CONVECTION HEAT TRANSFER OF POWER-LAW FLUIDS IN A VERTICAL ECCENTERIC ANNULUS

M. E. SAYED-AHMED

Department of Engineering, Mathematics and Physics, Faculty of Engineering, Cairo University, El-Fayoum Branch, El-Fayoum, Egypt

(*Received* 12 *October* 1998; *after revision* 4 *June* 1999; *Accepted* 12 *July* 1999)

A finite difference analysis has been made for the mixed convection heat transfer in a vertical stationary eccentric annulus for power law fluids. The nonlinear coupled momentum and energy equations have been solved using an iterative technique to obtain the velocity and temperature profiles. The outer surface of the annulus is considered to be adiabatic, while the inner surface has a uniform temperature. The average friction factor and average Nusselt number have been obtained for various values of Rayleigh number, model paraper and geometry parameters. The comparison of particular cases has been made are found in good agreement with the known results.

Key Words : Mixed Convection; Numerical Analysis; Non-Newtonian Fluids; Eccentric Annulus.

INTRODUCTION

Mixed convection heat transfer in a vertical annulus has been the subject of a great deal of attention because of many important engineering applications, such as in heat exchangers, nuclear reactors and the design of coolant channels for power transformers. However, under the real conditions, the cylinders of the annulus are often not concentric and therefore in an eccentric annulus, the flow characteristics must be evaluated using numerical methods. Many theoretical as well as experimental studies have been made for either pure forced convection or pure free convection. Very little has been known about combined free and forced convection heat transfer in a vertical eccentric annuli. In reality, pure forced convection heat transfer seldom occurs since density is dependent on temperature. Mixed convection, i.e., combined free and forced convection is the most general heat transfer phenomena. Pure free and pure forced convection are only limiting cases when either type of mixing motion can be neglected in comparison to the other (Kakac *et al.*[1]).

Many important industrial fluids are non-Newtonian in their flow characteristics and are referred to as rheological fluids. These include paints; various suspensions such as coal-water or coal-oil slurries, glues, inks, foods; polymer solutions; and many others. The rheology considered here, namely, the power-law, is the most frequently used in non-Newtonian fluid flow problems and can be used to represent the constitutive equation for cements and molten plastics, and polymer solutions.

For Newtonian fluid, laminar mixed convection in a vertical eccentric annulus has been studied by Sathyamurthy *et al.*[2]. They solved the equations governing the velocity and temperature by using a finite-volume technique under the thermal condition of uniform inner wall temperature

while the outer wall is insulated. Patel and Ingham[3] investigated the problem of mixed convection flow of a Bingham plastic in an eccentric annulus numerically using the finite element method and analytically using a narrow gap approximation. They assumed that the walls of the annulus are held at asymmetric constant temperature. Mixed convection heat transfer of a power-law fluid has been attempted by Shenoy[4] on a vertical plate and by Gori[5] in a long vertical tube. Patel and Ingham[6] studied the problem of mixed convection flow of a power-law fluid in parallel ducts analytically. Flow of a power-flaw fluid in an eccentric annulus has been attempted by Guckes[7] and Uner *et al.*[8]. The problem of the flow and forced convection heat transfer of a Sutterby fluid in an eccentric annulus has been studied by Batra and Eissa[9].

TABLE I

Comparison of the present results with those of Capobianchi and Irvine[11]

	Present results	Capobianchi and Irvine[11]	Present results	Capobianchi and Irvine[11]
		$n = 0.5$		
S	fRe	fRe	Nu	Nu
0.1	450.8977	451.2008	12.034	12.045
0.3	491.3882	491.7248	7.352	7.356
0.5	505.4652	505.6200	6.290	6.293
0.7	510.4834	510.7208	5.828	5.831
		$n = 1.5$		
0.1	51.2718	51.2613	11.793	11.826
0.3	52.9546	52.9436	7.159	7.172
0.5	53.4822	53.4736	6.116	6.124
0.7	53.6858	53.6855	5.6634	5.667

In this paper, we investigate the problem of mixed convection heat transfer of power-law fluids in a vertical eccentric annulus numerically by using a finite difference method. The outer surface of the annulus is considered to be adiabatic, while the inner surface has a uniform temperature. Velocity profiles, temperature distribution, friction factor and average Nusselt number have been obtained for various values of Rayleigh number, model parameter and geometry parameters.

MATHEMATICAL ANALYSIS

The problem being analyzed is that of steady state, fully developed, laminar, incompressible, combined free and forced convection in a vertical eccentric annulus. The geometry of eccentric annulus is shown in Fig. 1, where we have two infinitely long stationary vertical circular cylinders of radii R_1 and R_2 with centers set a distance d apart. The fluid properties are assumed to be constant except for the variation of density in the buoyancy term. The temperature of the inner wall is assumed to be uniform while the outer wall is insulated.

Under the above conditions and neglecting the viscous dissipation and compression work terms in the energy equation, equations governing the flow are

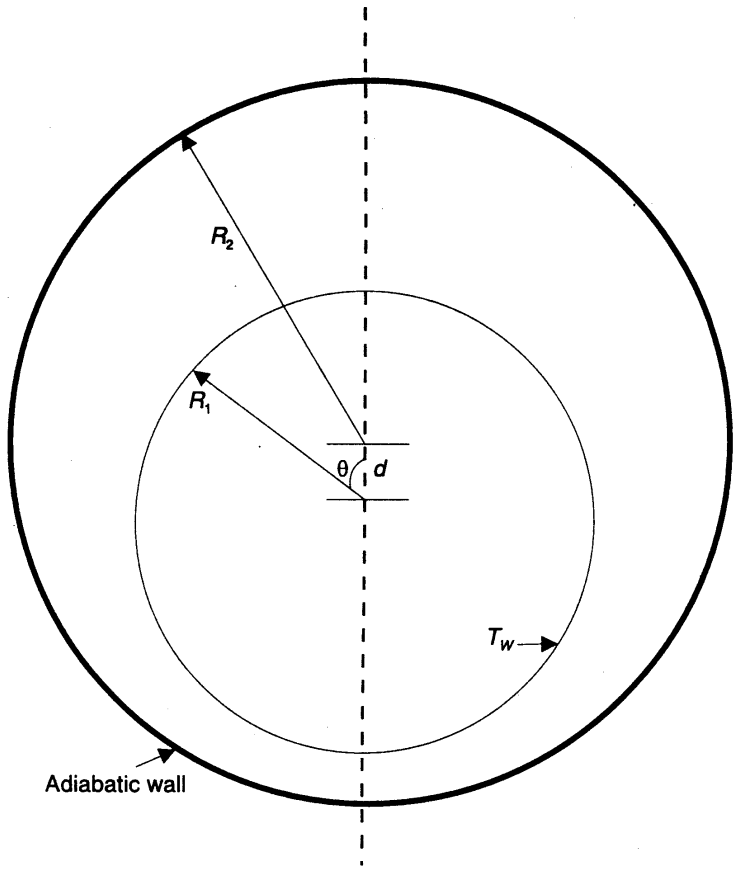

FIG. 1. An eccentric annulus

$$\frac{\partial}{\partial x}\left(\mu\frac{\partial v}{\partial x}\right)+\frac{\partial}{\partial y}\left(\mu\frac{\partial v}{\partial y}\right)=\frac{dp}{dz}+\rho g, \qquad \ldots (1)$$

and

$$\alpha\left(\frac{\partial^2 T}{\partial x^2}+\frac{\partial^2 T}{\partial y^2}\right)=v\frac{dT}{dz}, \qquad \ldots (2)$$

where v is the axial velocity, ρ is the density, p is the pressure, T is the temperature, α is the thermal diffusivity and μ is the apparent viscosity of the model and given by

$$\mu = m\left(\sqrt{\left(\frac{\partial v}{\partial x}\right)^2+\left(\frac{\partial v}{\partial y}\right)^2}\right)^{n-1}. \qquad \ldots (3)$$

Here, m is the consistency index of the model and n is the flow behaviour index. We take into consideration the effect of the density gradients resulting from the temperature variations by using Boussinesq approximation in the buoyancy term.

$$\rho = \rho_w\,[1+\beta(T_w - T)] \qquad \ldots (4)$$

where T_w is the temperature of the inner wall at any axial location, ρ_w the corresponding constant density at some reference location and β the coefficient of volumetric expansion. The temperature

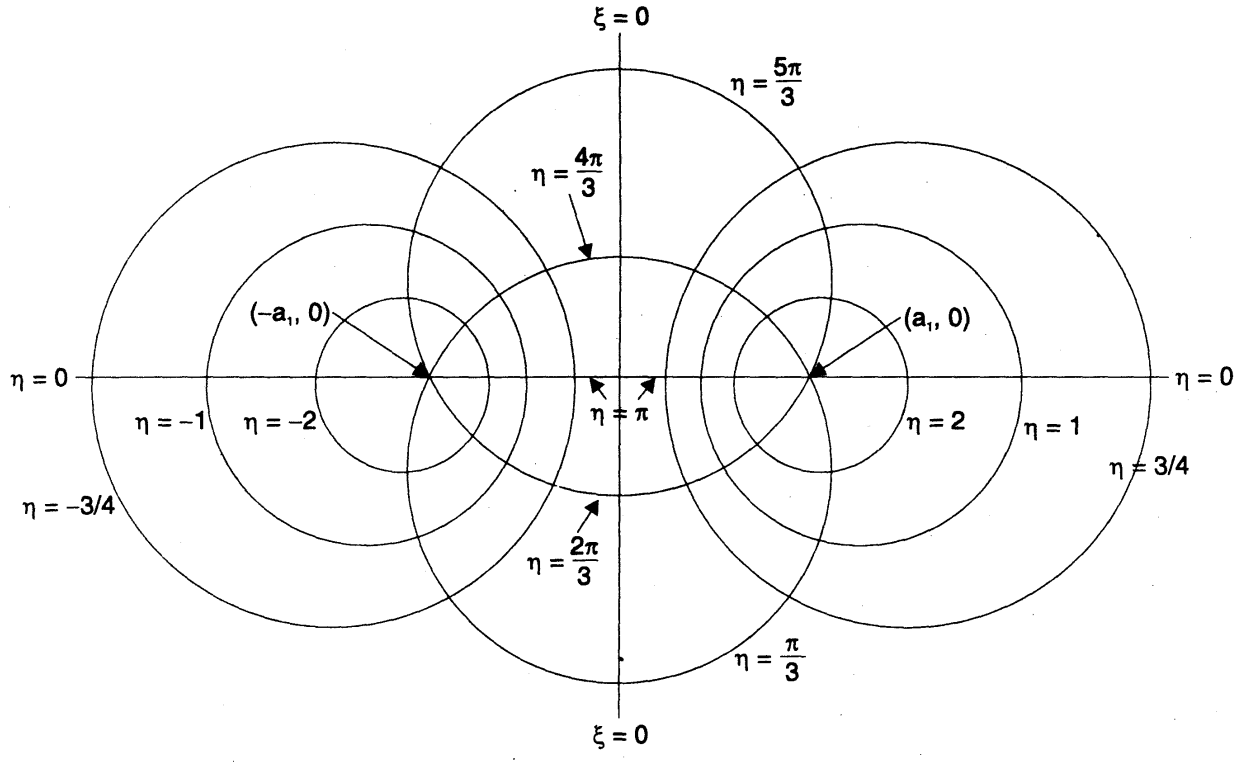

FIG. 2. Bipolar coordinate system

gradient $\frac{\partial T}{\partial z}$ can be written as (Sathyamurthy *et al.*[2])

$$\frac{\partial T}{\partial z} = \frac{Q}{\rho v_a A c_p}, \qquad \ldots (5)$$

where Q is the heat input per unit axial length, v_a the average axial velocity and A is the cross-sectional area of the annulus.

The handling of an eccentric annulus in a Cartesian coordinate system (x, y, z) can be very cumbersome, where as the bipolar coordinate system (ξ, η, z) consisting of two orthogonal systems of circles ξ and η, (Guckes[7]) provides an excellent alternative (Fig. 2). Making use of eqs. (4) and (5), eqs. (1), (2) and (3) in bipolar coordinates are given by

$$\left(\frac{\psi}{a}\right)^2\left[\frac{\partial}{\partial\xi}\left(\mu\frac{\partial v}{\partial\xi}\right)+\frac{\partial}{\partial\eta}\left(\mu\frac{\partial v}{\partial\eta}\right)\right]=\frac{dp}{dz}+\rho_w g\,[1+\beta(T_q-T)], \qquad \ldots (6)$$

$$\left(\frac{\psi}{a}\right)^2\left[\frac{\partial^2 T}{\partial\xi^2}+\frac{\partial^2 T}{\partial\eta^2}\right]=\frac{Q}{v_a A}v \qquad \ldots (7)$$

and

$$\mu = m\left|\frac{\psi}{a}\sqrt{\left(\frac{\partial v}{\partial\xi}\right)^2+\left(\frac{\partial v}{\partial\eta}\right)^1}\right|^{n-1}, \qquad \ldots (8)$$

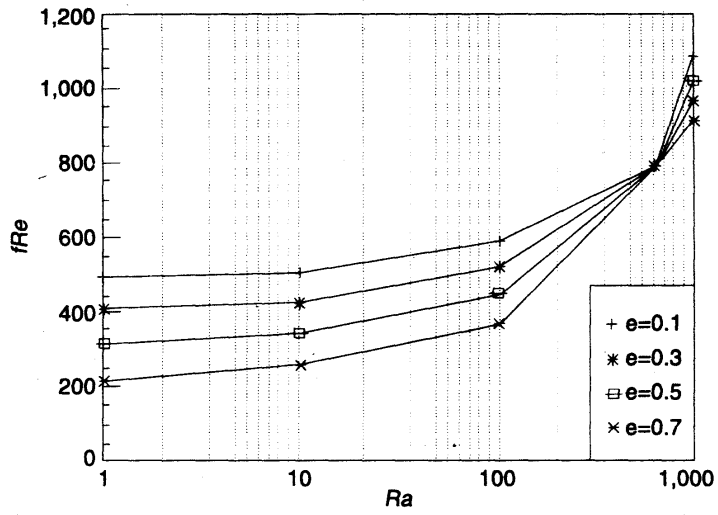

(a) n = 0.5

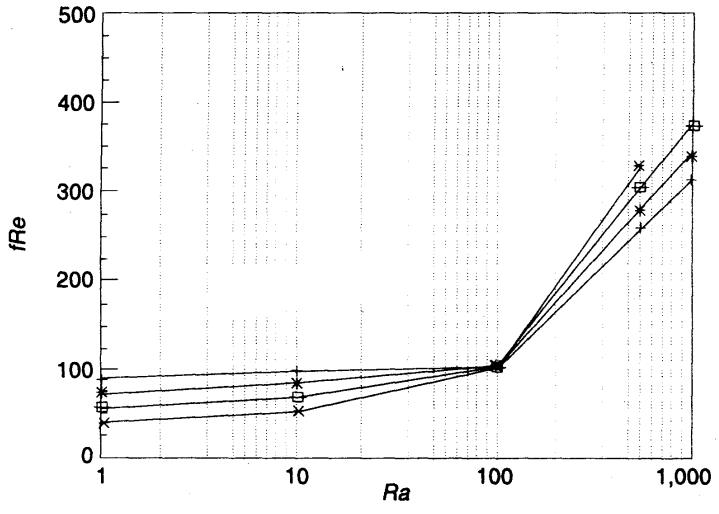

(b) n = 1.0

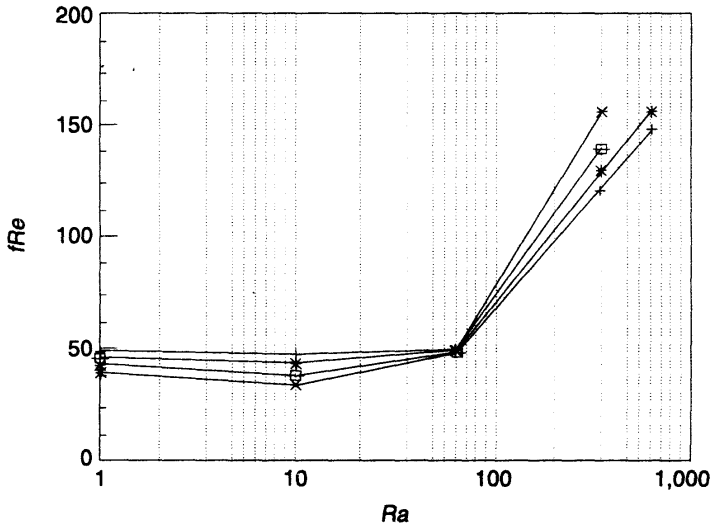

(c) n = 1.5

FIG. 3. The variation of the average friction number fRe with the Rayleigh number Ra for $S = 0.5$

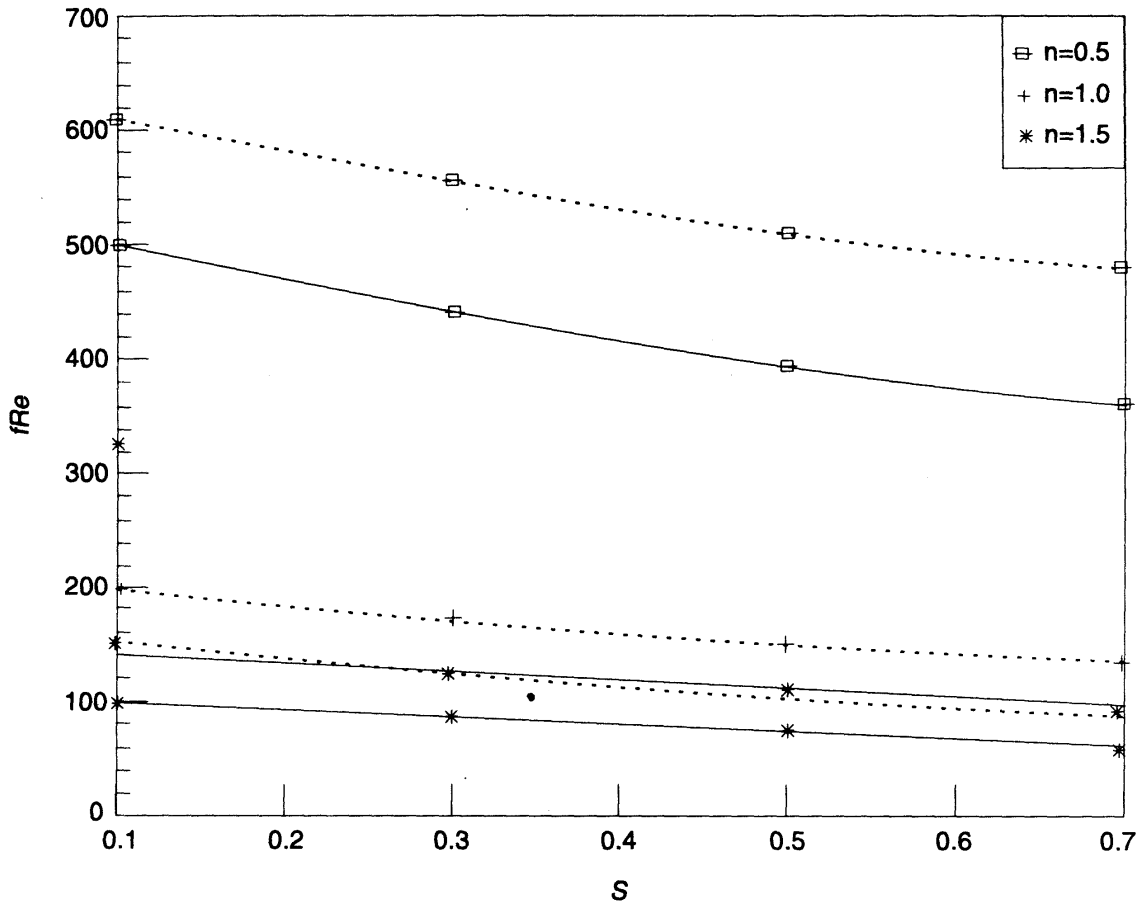

FIG. 4. The effect of the radius ratio S on the avarage friction number fRe for e = 0.5 Ra = 100 (—), 200 (···)

where $\psi = \cosh \xi - \cos \eta$ and $a = R_1 \sinh \xi_1 = R_2 \sinh \xi_2$.

The fluid motion is governed by the no-slip conditions at the inner and outer walls of the annulus and the symmetry conditions between the upper and lower halves of the annulus. The temperature at the inner wall is assumed to be a constant while the outer wall is insulated. These conditions are expressed as

$$\text{At } \xi = \xi_1,\ v = 0,\ T = T_w.$$

$$\text{At } \xi = \xi_2,\ v = 0,\ \frac{\partial T}{\partial \xi} = 0. \qquad \ldots (9)$$

Defining the dimensionless variables and parameters :

$$\bar{v} = \frac{v}{v_r},\ \bar{\mu} = \frac{\mu}{\mu_r},\ \bar{T} = \frac{T - T_w}{(QD_h^2)/(kA\bar{v}_a)},\ Ra = \frac{\rho_w \beta g D_h^4}{\alpha \mu_r}\left(\frac{\partial T}{\partial z}\right),$$

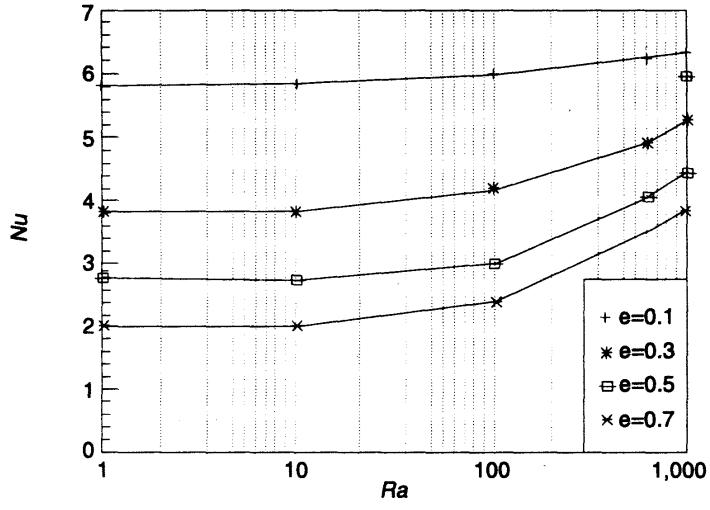

(a) n = 0.5

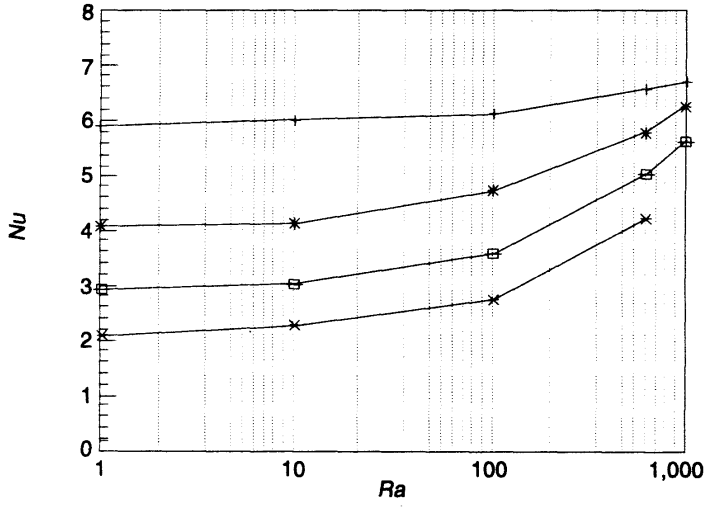

(b) n = 1.0

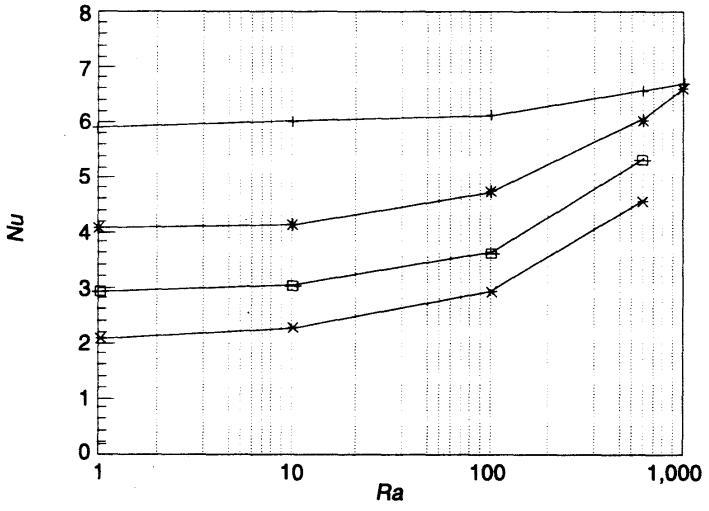

(c) n = 1.5

FIG. 5. The variation of the average Nusselt number Nu with the Rayleigh number Ra for $S = 0.5$

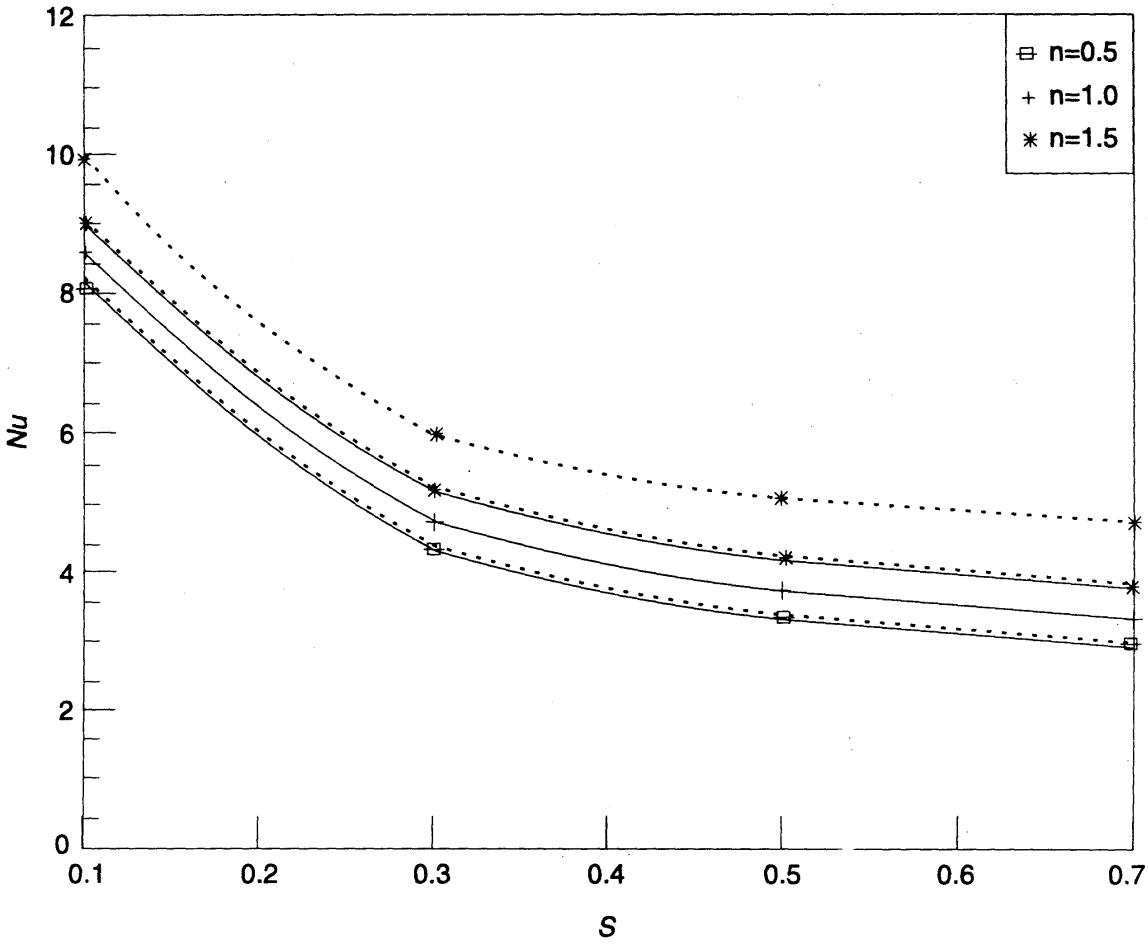

FIG. 6. The effect of the radius ratio S on the avarage Nusselt number Nu for e = 0.5 Ra = 100 (—), 200 (···)

$$f=\frac{D_h\left(-\frac{dp}{dz}-\rho_w g\right)}{\frac{1}{2}\rho_w v_a^2},\quad Re=\frac{\rho_w v_a D_h}{\mu_r},\quad S=\frac{R_1}{R_2},\quad e=\frac{d}{R_2-R_1},$$

where

$$v_r=\left[\left(-\frac{dp}{dz}-\rho_w g\right)\frac{D_h^{n+1}}{m}\right]^{1/n},\quad \mu_r=m\left(\frac{v_r}{D_h}\right)^{n-1},\quad D_h=2(R_2-R_1)$$

and

$$\bar{v}_a=\frac{2\sinh^2\xi_2}{\pi(1-S^2)}\int_0^{\pi}\int_{\xi_1}^{\xi_2}\frac{\bar{v}}{\psi^2}\,d\xi\,d\eta. \qquad \ldots (10)$$

Substituting the dimensionless variables into eqs. (6) and (7) gives the dimensionless form of the governing equations :

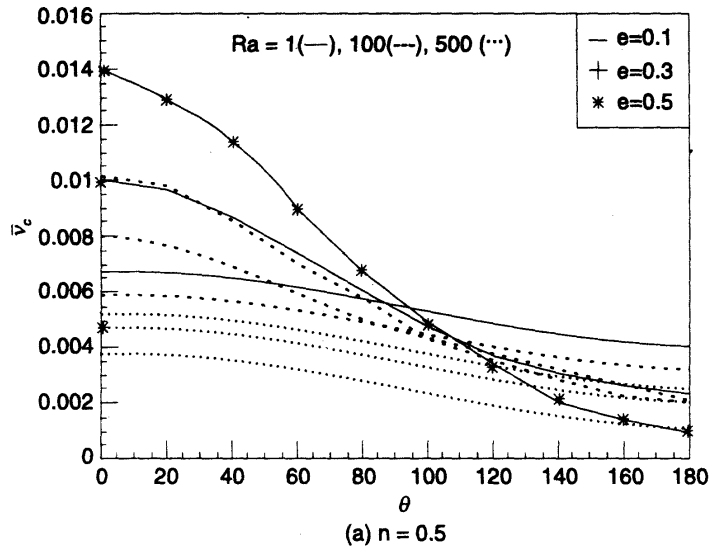

(a) n = 0.5

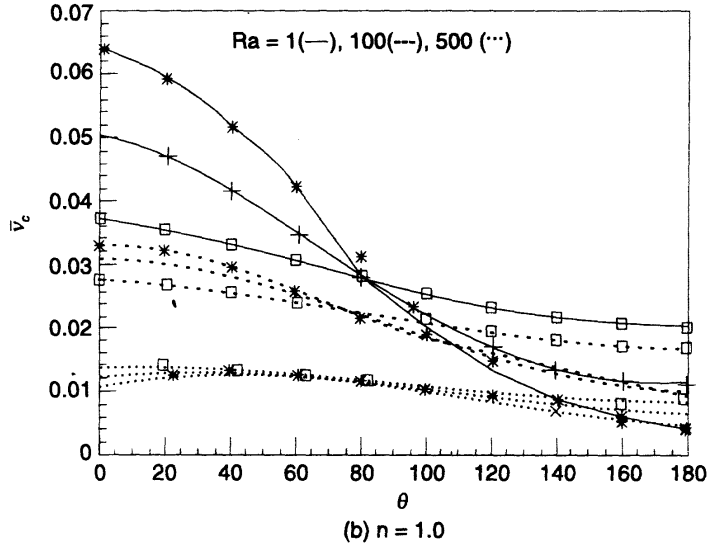

(b) n = 1.0

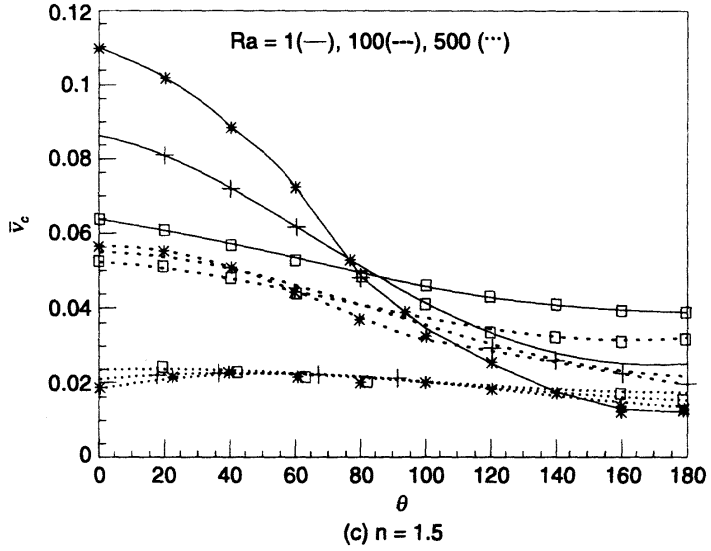

(c) n = 1.5

FIG. 7. The distribution of the centre line velocity $\bar{v}_c$ with the azimuthal direction θ for $S = 0.5$

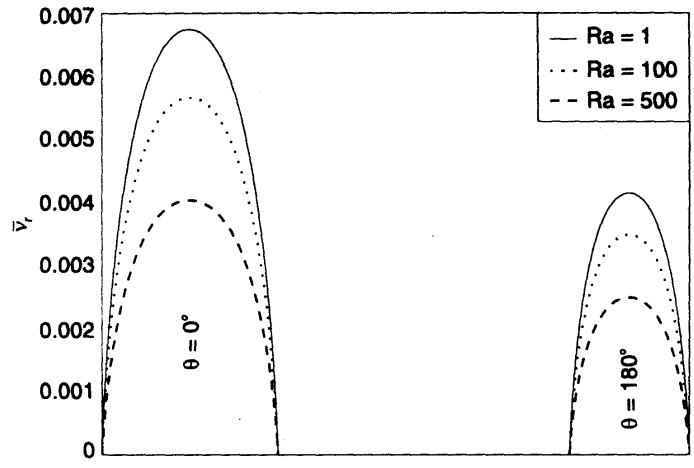

(a) n = 0.5

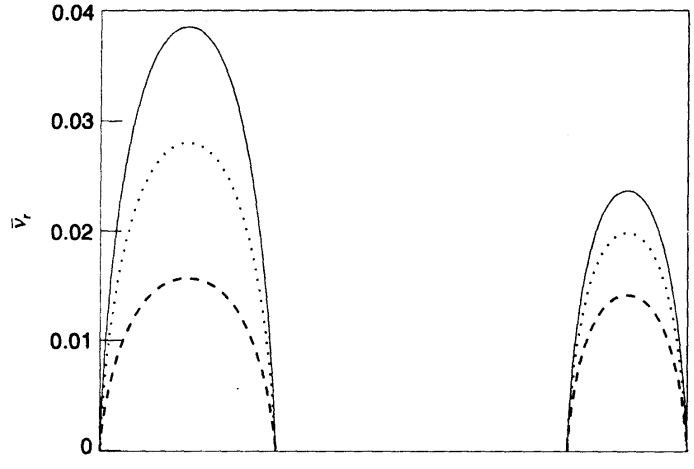

(b) n = 1.0

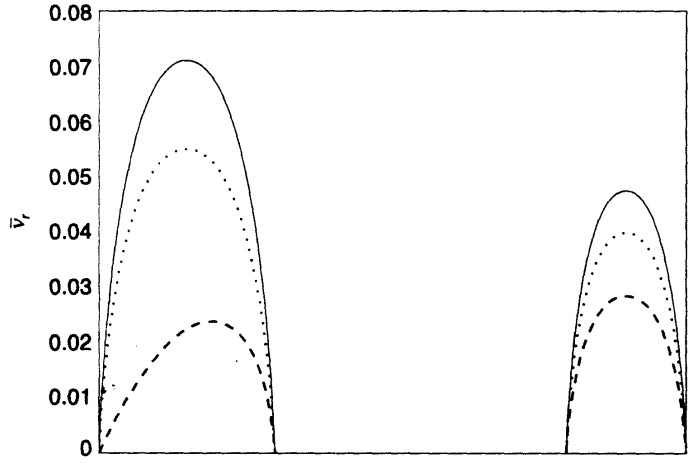

(c) n = 1.5

FIG. 8. The distribution of the radial velocity for $S = 0.5$ and $e = 0.1$

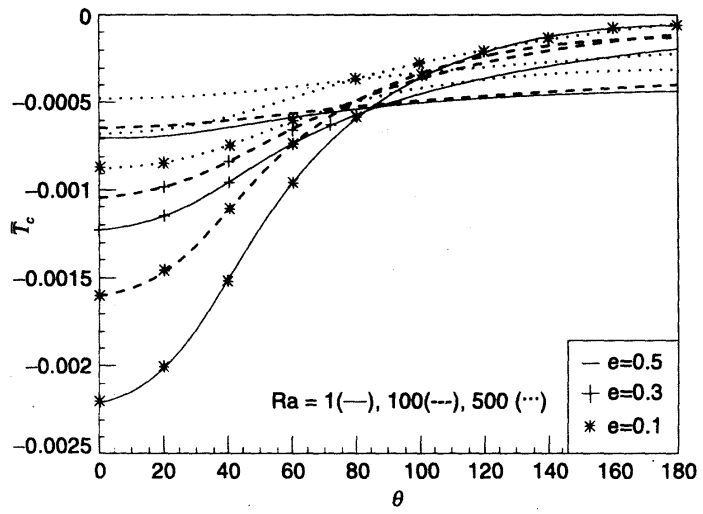

(a) n = 0.5

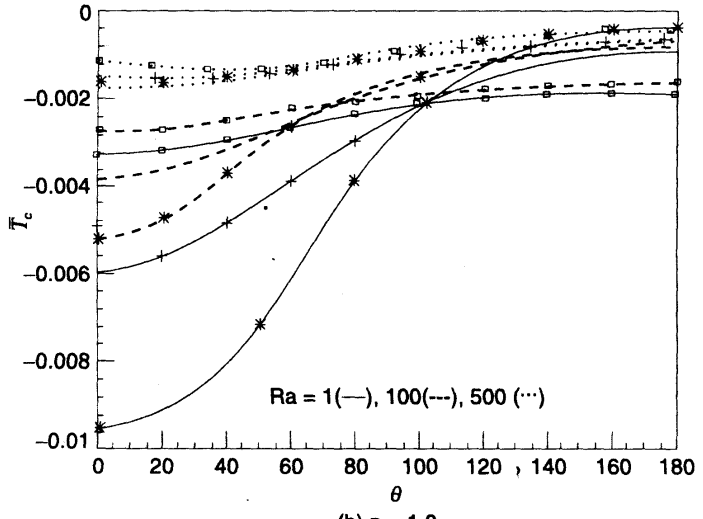

(b) n = 1.0

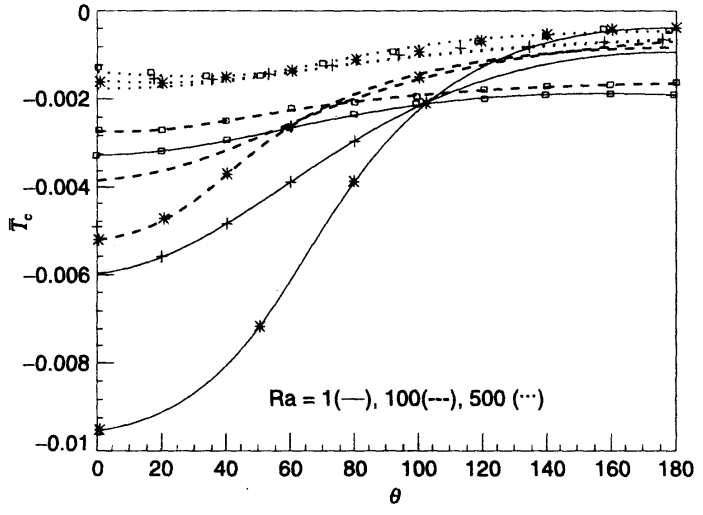

(c) n = 1.5

FIG. 9. The distribution of the centre line temperature $\bar{T}_c$ with the azimuthal direction θ for $S = 0.5$

$$\frac{\partial}{\partial\xi}\left(\bar{\mu}\frac{\partial\bar{v}}{d\xi}\right)+\frac{\partial}{\partial\eta}\left(\bar{\mu}\frac{\partial\bar{v}}{\partial\eta}\right)=-\left(\frac{\sinh\xi_2}{2\psi(1-S)}\right)^2(1+Ra\,\bar{T}), \qquad \ldots (11)$$

and

$$\frac{\partial^2\bar{T}}{\partial\xi^2}+\frac{\partial^2\bar{T}}{\partial\eta^2}=\left(\frac{\sinh\xi_2}{2\psi(1-s)}\right)^2\bar{v}, \qquad \ldots (12)$$

where

$$\bar{\mu}=\left|\frac{2(1-S)\psi}{\sinh\xi_2}\sqrt{\left(\frac{\partial\bar{v}}{\partial\xi}\right)^2+\left(\frac{\partial\bar{v}}{\partial\eta}\right)^2}\right|^{n-1}. \qquad \ldots (13)$$

The boundary conditions (9) in dimensionless form are

$$\text{At } \xi=\xi_1,\ \bar{v}=0,\ \bar{T}=0,$$

$$\text{At } \xi=\xi_2,\ \bar{v}=0,\ \frac{\partial\bar{T}}{\partial\xi}=0. \qquad \ldots (14)$$

NUMERICAL SOLUTION

The governing momentum and energy eqs. (11) and (12) were solved numerically by using the finite difference method. The annulus region is mapped by a grid of mesh points (ξ_i, η_j). $\Delta\xi$ and $\Delta\eta$ represent the uniform step lengths in the ξ and η direction respectively. Using central differences[10], eqs. (11) and (12) take respectively the form of difference equations,

$$\frac{\Delta\eta}{\Delta\xi}\left(\bar{\mu}_{i-1/2,\,j}\,\bar{v}_{i-1,j}+\bar{\mu}_{i+1/2\,j}\right)+\frac{\Delta\xi}{\Delta\eta}\left(\bar{\mu}_{i,\,j-\frac{1}{2}}+\bar{v}_{i,j-1}+\bar{\mu}_{i,j+1/2}\,\bar{v}_{i,j+1}\right)$$

$$-\left(\frac{\Delta\eta}{\Delta\xi}\left(\bar{\mu}_{i-1/2,j}+\bar{\mu}_{i+\frac{1}{2},j}\right)+\frac{\Delta\xi}{\Delta\eta}\left(\bar{\mu}_{i,\,j-\frac{1}{2}}+\bar{\mu}_{i,j+1/2}\right)\right)\bar{v}_{i,j}$$

$$+\ Ra\left(\frac{\sinh\xi_2}{2(1-S)\psi_{i,j}}\right)^2\Delta\xi\,\Delta\eta\,\bar{T}_{i,j}=-\left(\frac{\sinh\xi_2}{2(1-S)\psi_{i,j}}\right)^2\Delta\xi\,\Delta\eta \qquad \ldots (15)$$

$$\frac{\Delta\eta}{\Delta\xi}\left(\bar{T}_{i-1,j}+\bar{T}_{i+1,j}\right)+\frac{\Delta\xi}{\Delta\eta}\left(\bar{T}_{i,j-1}+\bar{T}_{i,j+1}\right)-2\left(\frac{\Delta\eta}{\Delta\xi}+\frac{\Delta\xi}{\Delta\eta}\right)\bar{T}_{i,j}$$

$$-\ \Delta\xi\,\Delta\eta\left(\frac{\sinh\xi_2}{2(1-S)\psi_{i,j}}\right)^2\bar{v}_{i,j}=0, \qquad \ldots (16)$$

where

$$\bar{\mu}_{i,j+1/2} = \left| \frac{2(1-S)\psi_{i,j+1/2}}{\sinh \xi_2} \sqrt{\left(\frac{\partial \bar{v}}{\partial \xi}\right)^2_{i,j+1/2} + \left(\frac{\partial \bar{v}}{\partial \eta}\right)^2_{i,j+1/2}} \right|^{n-1} \quad \ldots (17)$$

and $$\bar{\mu}_{i+1/2,j} = \left| \frac{2(1-S)\psi_{i+1/2,j}}{\sinh \xi_2} \sqrt{\left(\frac{\partial \bar{v}}{\partial \xi}\right)^2_{i+1/2,j} + \left(\frac{\partial \bar{v}}{\partial \eta}\right)^2_{i+1/2,j}} \right|^{n-1}, \quad \ldots (18)$$

and similar expressions for $\bar{\mu}_{i-1/2,j}$ and $\bar{\mu}_{i,j+1/2}$.

For the nonlinear coupled eqs. (15) and (16) an iterative procedure has been used since the apparent viscosity is a function of velocity gradients. The power-law fluid implies an infinite viscosity when the shear rate $\left(I = \sqrt{\left(\frac{\partial \bar{v}}{\partial \xi}\right)^2 + \left(\frac{\partial \bar{v}}{\partial \eta}\right)^2}\right)$ equals zero. This causes some computational difficulty which can be corrected by the addition a small constant ε to the shear rate to modify the viscosity of the model. The initial value for the viscosity is assumed to be constant (Newtonian viscosity) at each grid point. The coupled eqs. (15) and (16) with the differences form of the boundary conditions (14), are solved by the Successive Over-Relaxation method[10] to calculate the unknown velocity and temperature values. Making use of these values, a new value of the apparent viscosity is obtained from the difference form of eqs. (17) and (18). The process is repeated up till the criteria of convergence $\left| \frac{\bar{\mu}^{new}_{i,j} - \bar{u}^{old}_{i,j}}{u^{new}_{i,j}} \right| \leq 10^{-5}$ and $\left| \frac{\bar{T}^{new}_{i,j} - \bar{T}^{old}_{i,j}}{T^{new}_{i,j}} \right| \leq 10^{-5}$ is satisfied. The convergence is achieved by taking 100 × 100 mesh points for both hydrodynamic and thermal parts and $\varepsilon = 10^{-8}$.

The *fRe* factor is defined as the product of the fanning friction factor f (the ratio of the pressure energy to the kinetic energy per unit volume) and the Reynolds number for the model *Re* and given by

$$fRe = \frac{2}{\bar{v}_a}. \quad \ldots (19)$$

The average Nusselt number *Nu* at the inner wall is given by

$$Nu = -\frac{(1+S)\bar{v}_a}{4S\,\bar{T}_m}, \quad \ldots (20)$$

where $\bar{T}_m$ is the mean fluid temperature given as

$$\bar{T}_m = \frac{2\sinh^2 \xi_2}{\pi(1-S^2)\,\bar{v}_a} \int_0^{\pi} \int_{\xi_1}^{\xi_2} \frac{\bar{u}\,T}{\psi^2}\, d\xi\, d\eta. \quad \ldots (21)$$

The above definite double integrals in eqs. (10) and (21) are evaluated numerically using Simpson's 1/3 rule[9]. Then the average frition factor and Nusselt number can be estimated from eqs. (19) and (20).

RESULTS AND DISCUSSION

A finite difference solution has been obtained for the mixed convection heat transfer in a vertical eccentric annulus for power law fluids. The coupled momentum and energy equations have been solved using an iterative technique to obtain the velocity and temperature profiles. Computations have been obtained for various values of the Rayleigh number, eccentricity e, radius ratio S and flow behaviour index n.

The distribution of the average friction factor fRe with the Rayleigh number Ra is shown in Fig. 3(a, b, c) for radius ratio $S = 0.5$, different values of eccentricity e and flow index $n = 0.5$, 1 and 1.5, respectively. For each case, the Rayleigh number is limited by the critical value beyond which reverse flow will occur. The effect of radius ratio S on the friction factor fRe is shown in Fig. 4 for $e = 0.5$, $Ra = 100$ and 200 and the same above values of n. Examination of these Figures shows that the value of fRe increases with the increase of Ra for all values of e and n. The increase in the value of e decreases fRe up to some value of Ra (say Ra_1), then beyond Ra_1 the effect is reversed for all values of n and the value of Ra_1 decreases with increase of n. This behavior can be understood by noting that for forced convection ($Ra = 0$), the increase in the value of eccentricity increases the average velocity and hence reduces the factor fRe. However, the increase in Ra reduces the maximum velocity in the wide part of the annulus and the average velocity. Therefore, the value of fRe increases with the increase in e and hence the effect of the Rayleigh number on fRe is stronger than the effect of eccentricity. Also, it has been noted that the value of fRe increases suddenly for large values of Ra. The value of fRe decreases with increase in S and n. It has been found that the critical Rayleigh number decreases with the increase in within the values of n and e.

The effect of buoyancy force which is characterized by Ra on the average Nusselt number Nu for $e = 0.1$, 0.3, 0.5, 0.7 and $n = 0.5$, 1.0, 1.5 is shown in Fig. 5 (a, b, c) respectively. Fig. 6 shows the effect of radius ratio S on Nu for $e = 0.5$, $n = 0.5$, 1.0, 1.5 and $Ra = 100$ and 200. The study of these figures shows that the value of Nu increases with Ra for all values of n and e. The increase in the value of e decreases the value of Nu due to an increase in the area of low resistance and consequently, the fluid flows in the region of the widest annular gap. Therefore, at a given Rayleigh number, larger eccentricities lead to greater nonuniformities in the velocity and temperature profiles. Also, the value of Nu increases with n for all value of e and Ra. The effect of Ra in Nu decreases with S for all values of n. The Rayleigh number at which the buoyancy forces begin to affect the flow and heat transfer parameters is greater or equal to the value of Ra_1 for all values of n.

The distribution of the centre line velocity with θ (where ∂ is the polar angle of the central circle and is given by $\partial = \tan^{-1}((\sinh \xi_1 \sin \eta)/(\cosh \xi_1 \cos \eta - 1))$) for $S = 0.5$, $e = 0.1$, 0.3, 0.5, different values of Ra and $n = 0.5$, 1, 1.5 is shown in Figs. 7 (a, b, c) respectively. For $Ra = 1$, 100, 500, $e = 0.1$, $S = 0.5$ and the same above values of n, the distribution of the radial velocity is shown in Figs. 8 (a, b, c) for $\theta = 0^\circ$ and 180°. It has been found that, the centre line velocity decreases with θ for $n < 1$ (shear thinning fluid) and for all values of Ra. However, for $n = 1$ (Newtonian fluid) and $n > 1$ (shear-thickening fluid), the centre line velocity decreases with θ for small values of Ra, but for large value of Ra, it increases with θ for θ varies from 0° to 80° and with reversed effect for θ varies from 80° to 180°. The increase in the value of Ra decreases the

value of the centre line velocity for all n. The value of $\overline{v}_c$ increases with e in the wide part of the annulus (near $\theta = 0^o$) and it decreases with e in the narrow part of the annulus (near $\theta = 180^o$). The increase in the value of n increases the value of $\overline{v}_c$. For large value of Ra and small value of e, the variation of $\overline{v}_c$ with θ is negligible. Also, the maximum value of the velocity decreases with Ra and the location of the maximum velocity is shifted away from the symmetry line through the widest gap and toward the region of smaller clearance gap. It has been noted that, the maximum value of the velocity is greater in the wide part of the annulus than it in the narrow part because for a given pressure gradient. Increasing the value of Ra, the maximum value of the velocity decreases more in the wide part than in the narrow part of the annulus. However, for large value of Ra, the distribution of the radial velocity is uniform for all values of n. Also, the distribution of the radial velocity is flatter for small value of n (shear-thinning fluid).

The variation of the centre line temperature with θ is shown in Figs. 9 (a, b, c) for S = 0.5, n = 0.5, 1.0, 1.5 and different values of Ra and e. It has been observed that the value of the temperature increases with θ for all values of n and e. The increase in the value of e decreases the temperature $\overline{T}_c$ in the wide part of the annulus and increases it in the narrow part of the annulus. Also, the temperature $\overline{T}_c$ increases with the increase in the value of Ra. It has been found that for large value of Ra, the effect of the eccentricity e on the temperature can be neglected for all values of n.

The present results have been found in well agreement with those obtained by Sathyamurthy *et al.*[2] for the particular case n = 1 (Newtonian fluid). Also, for e = 0 and Ra = 0, the present numerical results have been compared with the results of forced convection of power law fluid in concentric annuli obtained by Capobianchi and irvine[11] and are found in good agreement as shown in Table I.

CONCLUSIONS

The problem of mixed convection heat transfer of power law fluid in a vertical eccentric annulus has been investigated using a finite difference technique. The coupled momentum and energy equations have been solved using an iterative technique to obtain the velocity and temperature profiles. Computations have been obtained for a various values of Rayleigh number, eccentricity, radius ratio and flow behavior index. For all values of e and S, the friction factor and Nusselt number each increases with the Rayleigh number. The increase in the value of flow behavior index decreases the friction factor and increases the Nusselt number. The effect of the buoyancy forces is more significant for large values of eccentricity and flow index. It has been observed that, the Rayleigh number at which the buoyancy forces begin to affect the flow and heat transfer parameters is greater than or equal the value of Ra_1 which beyond it the effect eccentricity on friction factor is reversed for all values of n. For all values of n, the velocity profile is uniform for large values of Rayleigh number and it is flatter for shear-thinning fluids.

REFERENCES

1. S. Kakac, R. K. Shah and W. Aung, *Handbook of Single-Phase Convective Heat Transfer*, Wiley, New York (1987), Chapter 15.
2. P. Sathyamurthy, K. C. Karki and S. V. Patankar, *Numer. Heat Transfer, Part A*, **22** (1992) 71.
3. N. Patel and D. B. Ingham, *Int. J. Heat Fluid Flow*, **15** (1994) No. 2, 132.
4. A. V. Shenoy, *AIChE J.*, **26** (1980) 505.

5. F. Gori, *J. Heat Transfer*, **100** (1978) 220.
6. N. Patel and D. B. Ingham, *Int. Comm. Heat Mass Transfer*, **21** (1994) 75.
7. T. L. Guckes, *Trans ASME, J. Engng. Ind.* **97** (1975) 498.
8. D. Uner, C. Ozgen and I. Tosun, *Ind. Engng chem Res.*, **27** (1988) 678.
9. R. L. Batra and M. Eissa, *Mech. Res. Commun.* **21** (1994) No. 20, 147.
10. H. M. Antia, *Numerical Methods for Scientists and Engineers*, Tata McGraw-Hill, New Delhi, (1991).
11. M. Capobianchi and T. F. Jr. Irvine, *Warme-und Stoffubertragung*, **27** (1992) 209.